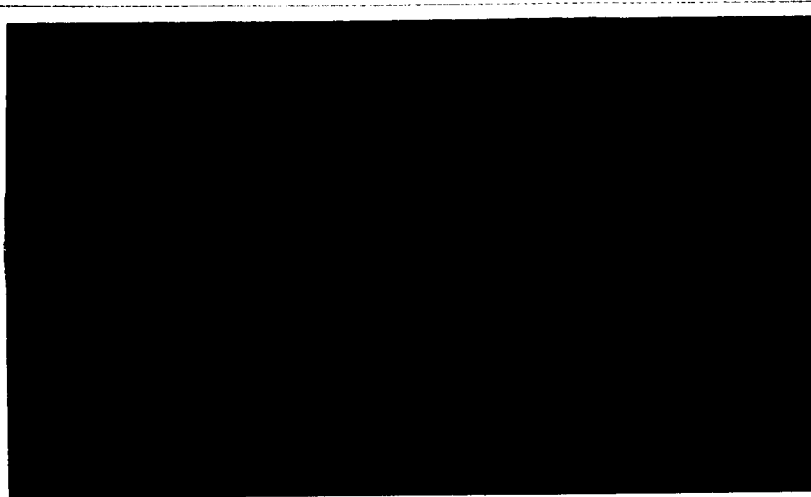
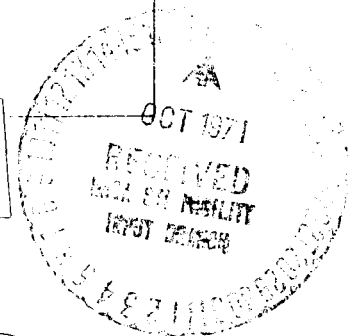


2-P

RESEARCH REPORT



Reproduced by
**NATIONAL TECHNICAL
INFORMATION SERVICE**
U S Department of Commerce
Springfield VA 22151



N72-12456 (NASA-CR-124613) *X* *No AD* THE EFFECT OF ALLOY
COMPOSITION ON THE MECHANISM OF STRESS
CORROSION CRACKING OF TITANIUM ALLOYS IN
AQUEOUS D.N. Williams (Battelle Memorial
Inst.) Oct. 1971 23 p
Unclas 08984 (NASA CR OR TMX OR AD NUMBER) CACL 11F G3/17

QUARTERLY PROGRESS REPORT

(June 11, 1971 - September 11, 1971)

on

THE EFFECT OF ALLOY COMPOSITION ON
THE MECHANISM OF STRESS-CORROSION
CRACKING OF TITANIUM ALLOYS IN
AQUEOUS ENVIRONMENTS

to

NATIONAL AERONAUTICS AND
SPACE ADMINISTRATION
Contract No. NASW-2242

October 1971

by

D. N. Williams, R. A. Wood, J. D. Boyd,
and R. I. Jaffee

BATTELLE
Columbus Laboratories
505 King Avenue
Columbus, Ohio 43201

G1265-1 OK'd by H. R. Ogden, D. N. Williams, R. A. Wood,
J. D. Boyd, and R. I. Jaffee before typing.

cc: R. I. Jaffee D. N. Williams Contracts Files
 H. R. Ogden R. A. Wood MSG Report Files
 J. D. Boyd W. K. Boyd Chrono

 **Battelle**
Columbus Laboratories
505 King Avenue
Columbus, Ohio 43201
Telephone (614) 299-3151
Telex 24-5454

October 12, 1971

National Aeronautics and Space Administration
Scientific and Technical Information Facility
P. O. Box 33
College Park, Maryland 20740

Gentlemen:

Contract NASW-2242

Enclosed are three copies, one of which is reproducible, of the First Quarterly Progress Report on the above contract entitled "The Effect of Alloy Composition on the Mechanism of Stress-Corrosion Cracking of Titanium Alloys in Aqueous Environments". Additional copies have been distributed as indicated below.

Very truly yours,

R. I. Jaffee
Project Coordinator

RIJ/jbs
Enc.

cc: NASA Headquarters
 Washington, D. C. 20546
 Attn: New Technology Representative,
 Code: KT

NASA Headquarters
 Washington, D. C. 20546
 Attn: Mr. Richard Raring, Code RWM

TABLE OF CONTENTS

	<u>Page</u>
INTRODUCTION	1
EFFECTS OF ALLOY COMPOSITION ON SUSCEPTIBILITY	1
Preparation of Experimental Alloys	1
Saltwater Stress Corrosion in Low-Aluminum Titanium- Aluminum Alloys	2
METALLURGICAL MECHANISMS OF STRESS-CORROSION CRACKING	19
REFERENCES	19

THE EFFECT OF ALLOY COMPOSITION ON
THE MECHANISM OF STRESS-CORROSION
CRACKING OF TITANIUM ALLOYS IN
AQUEOUS ENVIRONMENTS

by

D. N. Williams, R. A. Wood, J. D. Boyd,
and R. I. Jaffee

INTRODUCTION

This research program is concerned with the effects of alloy composition on the aqueous stress corrosion of titanium alloys. Emphasis is being placed on determining the interrelations among the composition, phase structure, and deformation and fracture properties of the alpha phase in susceptible alpha-beta alloys. The program is divided into two parts. The first consists of evaluating the aqueous stress-corrosion susceptibility of a series of alloys that contain various alpha-soluble elements. The second consists of an investigation of the metallurgical aspects of the mechanism of aqueous stress-corrosion cracking. During the first quarter of the contract period, work has progressed simultaneously on both parts of the research program. Significant accomplishments are summarized below.

EFFECTS OF ALLOY COMPOSITION
ON SUSCEPTIBILITY

Preparation of Experimental Alloys

Seven ingots weighing approximately 5.4 kilograms (12 pounds)* each were purchased from Titanium Metals Corporation. The nominal compositions of these ingots are as follows:

Ti-5Al-6Sn-1.5Mo-0.5V-0.1 O₂
Ti-5Al-6Ga-1.5Mo-0.5V-0.1 O₂
Ti-5Al-6In-1.5Mo-0.5V-0.1 O₂
Ti-5Al-10Zr-1.5Mo-0.5V-0.1 O₂
Ti-6Al-5Ta-1.5Mo-0.5V-0.1 O₂
Ti-6Al-3Cb-1.5Mo-0.5V-0.1 O₂
Ti-8Al-0.1 O₂

These alloys will be used to extend our investigation of the effects of composition on stress-corrosion susceptibility and to provide additional material for use in the study of mechanisms of stress corrosion. The ingots are being readied for fabrication to plate.

*The present study is conducted using standard English units. Conversion to SI units is done in the report in compliance with contract requirements.

A section of 6-cm-thick rolled plate of the Ti-4Al-3Mo-1V composition was provided at no cost by the Titanium Metals Corporation for use in studies of the effects of thickness (stress distribution) on stress-corrosion behavior of moderate-strength, high-toughness titanium alloys. This plate is being sectioned to provide samples for evaluation.

Saltwater Stress Corrosion in Low-Aluminum Titanium-Aluminum Alloys

A number of fatigue-cracked 6.34-mm- (0.25-inch) wide samples* of Ti-4Al-1.5Mo-0.5V and Ti-4Al-3Mo-1V alloys were available from previous work on Contract NASr-100(09). The yield strengths of these alloys were such that valid determinations of $K_{I_{SCC}}$ with samples as thin as 6.34 millimeters (0.25 inch) could not be expected unless $K_{I_{SCC}}$ was as low as the calculated $K_{I_{SCC}}$ values shown below:

	Yield Strength		Maximum Measurable $K_{I_{SCC}}$ *	
	N/m^2	Ksi	$MN/m^{3/2}$	$Ksi-In.^{1/2}$
Ti-4Al-1.5Mo-0.5V	703	102	35	32
Ti-4Al-3Mo-1V	785	114	40	36

Although low-aluminum titanium-aluminum alloys are not considered especially sensitive to saltwater stress corrosion, it was considered probable that these samples could provide useful data regarding several unresolved questions relative to the stress-corrosion behavior of titanium alloys in saltwater.

Foremost among these questions was uncertainty regarding the occurrence of a limited amount of subcritical crack growth followed by crack arrest in samples susceptible to stress corrosion but loaded such that plane stress conditions soon were dominant at the crack front. Second, it was desired to determine whether crack growth always occurred immediately upon loading or whether a finite crack initiation or delay time occurred. Third, the behavior of samples in prolonged static loading was of interest, especially the extent to which creep interacted with crack growth. Finally, it was of interest to determine if saltwater stress corrosion sensitivity could be detected in low-to-moderate-strength alloys with samples as thin as 6.34 meters (0.25 inch).

Ten samples of Ti-4Al-3Mo-1V alloy and twelve samples of Ti-4Al-1.5Mo-0.5V alloy were available for examination. All were 6.34 millimeters (0.25 inch) thick by 25.4 millimeters (1.0 inch) wide and had been fatigue cracked to a depth of 7.61 millimeters (0.23 to 0.30 inch) approximately 14 months previously. These samples were stressed at constant load in cantilever bending using our standard techniques.

Two methods were used to detect crack movement under constant load. In the first, a dial gage was attached to the lever arm approximately 0.6 meter (2 feet) from the crack location, and the lever arm deflection was measured at intervals throughout

*From the relationship $t \geq 2.5 \left(\frac{K}{Y_S} \right)^2$.

the period under load. The type of deflection:time behavior observed is shown in Figure 1, in which data are shown for three Ti-4Al-1.5Mo-0.5V alloy samples. Several comments of interest can be made regarding these curves:

- (a) In the absence of crack growth, a linear relationship is observed between lever arm deflection and log time. This deflection is apparently the result of creep. All samples tested showed creep, even at the lowest stress-intensity examined, $39 \text{ MN/m}^{3/2}$ ($35 \text{ ksi-in.}^{1/2}$). Creep behavior can be compared, qualitatively at least, on the basis of the slope of the deflection:log time curve.
- (b) Crack initiation (C. I.) is indicated by an increase in slope of the deflection:log time curve. In most cases, crack initiation occurred within 10 minutes after load application although, in several instances - usually, in tests at low stress intensities - crack initiation occurred only after several hours under load.
- (c) Crack arrest (C. A.) was indicated (apparently) by a return to a linear deflection:log time relationship. Crack arrest occurred anywhere from 20 to 3000 minutes after load application in the samples tested. In some cases, crack growth was still indicated after 10,000 minutes under load.
- (d) The increase in lever arm deflection, as compared with the expected deflection based upon extrapolation of behavior prior to crack initiation, provides a means of comparing amounts of crack growth:

	Deflection in 10^4 Min				Increase in Deflection, $\frac{D_A - D_E}{D_E}$
	Expected, D_E		Actual, D_A		
	Millimeters	Mils	Millimeters, $\times 10^4$	Mils	
72-2	0.685	27.6	1.852	73.0	1.7
72-1	0.642	25.3	0.990	39.0	0.5
72-C	0.338	13.3	0.338	13.3	0

In the second method of detecting crack growth, a dye was placed in the crack opening at the conclusion of the loading period, following which the sample was broken by manually depressing the lever arm. The location of the dye in the crack front was observed visually. In the case of tests in saltwater, the saltwater was removed and the sample dried before dye was applied. The characteristic of this method to show crack movement is illustrated in Figure 2. It is relatively easy to distinguish the interface between the fatigue crack and the crack grown under static load, and the interface between the crack grown under static load and the onset of rapid fracture induced manually is also obvious. In all cases examined, a marked tunnelling during slow crack growth was observed. In only two samples, 72-3 (shown in Figure 2) and 70-1, was any crack movement noted on the surface, and in these cases the surface crack extension was only 0.5 to 1.0 millimeter (0.02 to 0.04 inch). Surface crack growth undoubtedly occurred in Sample 70-4, which failed under constant load, but it was not detected at the last reading interval prior to failure. The two samples shown in Figure 2, a. and b., represent samples whose deflection:time behavior was reproduced in Figure 1. The correlation of maximum crack depth as determined using a marker dye with increase in lever-arm deflection is shown below.

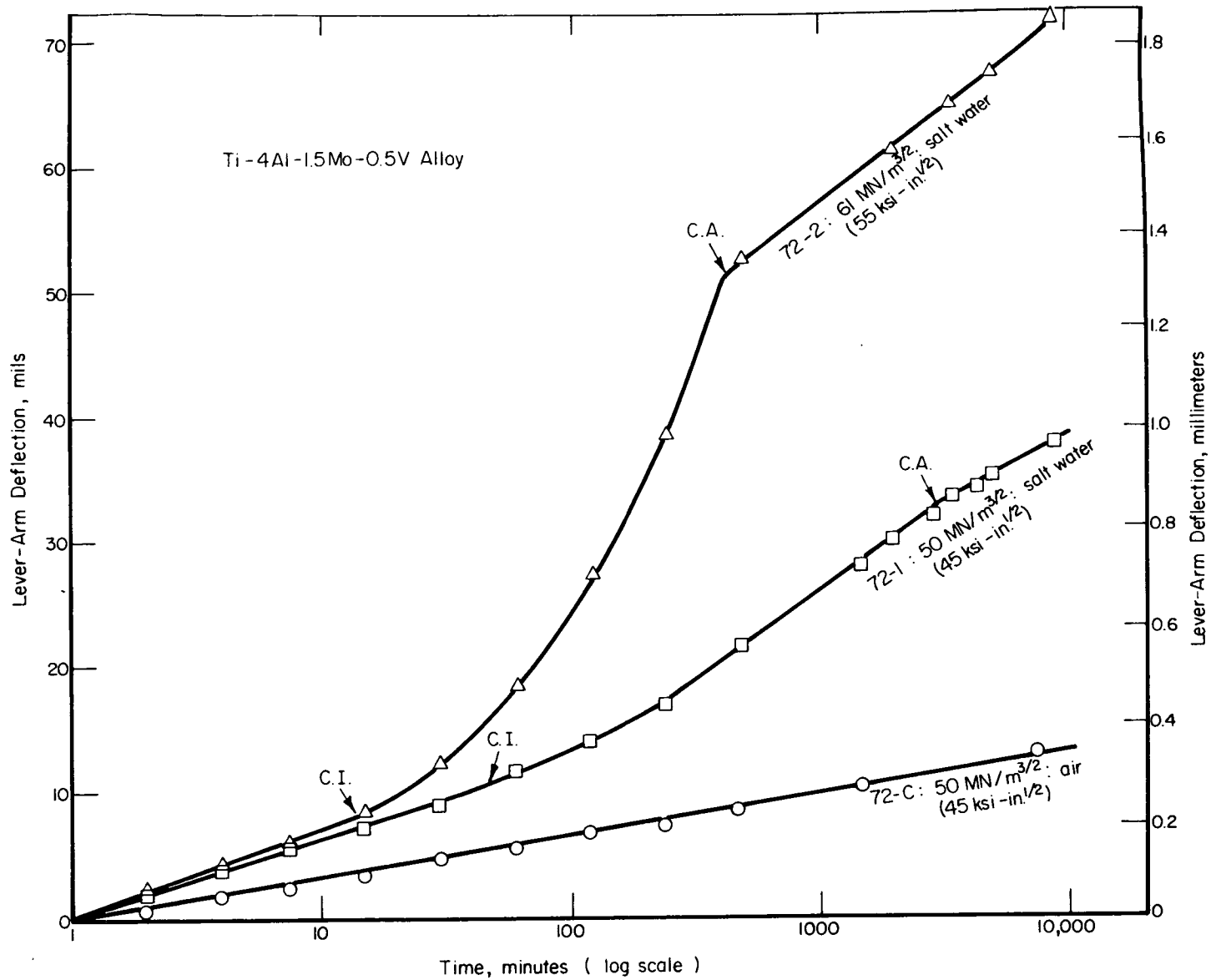
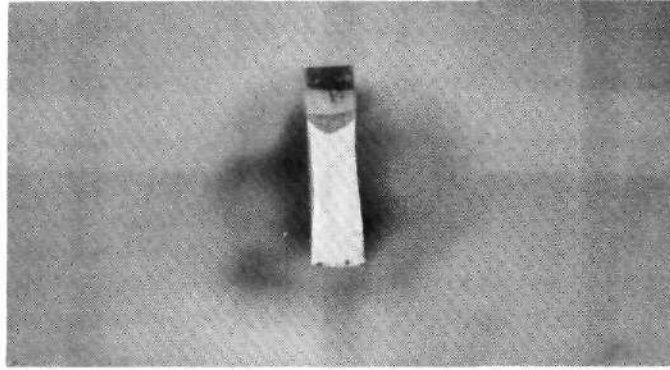
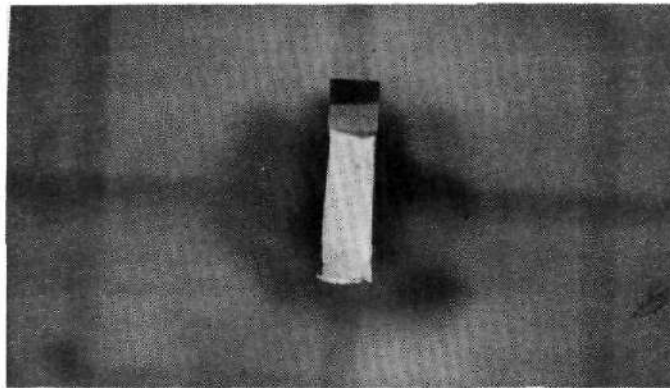


FIGURE 1. LEVER-ARM DEFLECTION AS A FUNCTION OF TIME AT CONSTANT LOAD
 C.I. = crack initiation; C.A. = crack arrest.



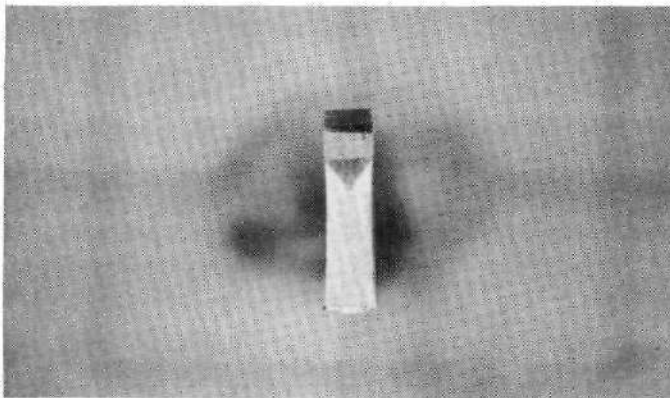
1X

a. Sample 72-2, $61 \text{ MN/m}^{3/2}$ ($55 \text{ ksi-in.}^{1/2}$) in Saltwater



1X

b. Sample 72-1, $50 \text{ MN/m}^{3/2}$ ($45 \text{ ksi-in.}^{1/2}$) in Saltwater



1X

c. Sample 72-3, $72 \text{ MN/m}^{3/2}$ ($65 \text{ ksi-in.}^{1/2}$) in Air

NOT REPRODUCIBLE

FIGURE 2. PHOTOGRAPHS OF THREE SAMPLES AFTER DYE MARKING OF CRACK FRONT AND MANUAL FRACTURING

	Maximum Crack Depth		Increase in Lever-Arm Deflection, 10^4 Minutes
	Millimeters	Inch	
72-2	2.5	0.10	1.7
72-1	1.0	0.04	0.5

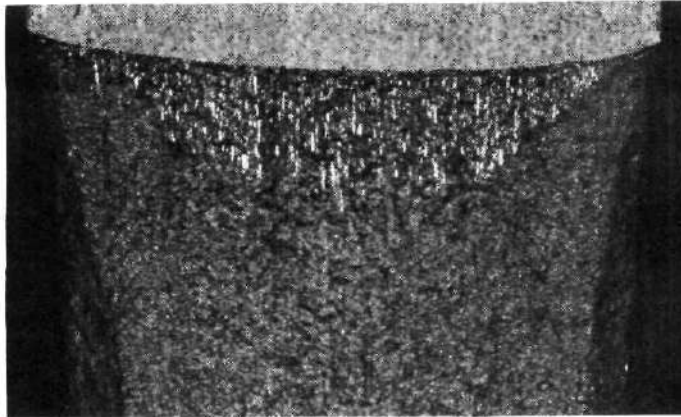
The dye marking technique required careful experimental technique to avoid dye movement during rapid fracture. Turco Dy-Chek dye penetrant proved to be the best marking material of those examined since it penetrated well, without itself introducing additional stress-corrosion cracking. All excess dye had to be removed (by use of compressed air and by judicious heating of the sample) to prevent dye creep onto the surface during fast fracture.

Macroscopic examination of fractured samples also provided an indication of crack movement, since the fracture surface was found to have a distinctive appearance in regions showing slow crack growth. Macrophotographs of three fracture surfaces are shown in Figure 3. The upper two photographs show samples which developed cracks under constant load in saltwater and in air. The region of slow crack growth is made visible by the presence of reflective-appearing planar facets. Correlation of the faceted regions with marker-dye patterns showed them to be quite similar in shape and in extent. The fast fracture region was much grainier appearing and was free of these facets. Samples fractured in seawater by step loading showed another distinguishing feature as shown in Figure 3c, with secondary cracks running into the sample along a plane perpendicular to the fracture plane and containing the direction of slow crack growth (vertical in Figure 3). These cracks appear as short, dark lines clustered fairly close to the boundary separating the region of slow crack growth from the region of fast fracture accompanying final failure. The sample shown in Figure 3c also exhibited a considerable number of reflecting facets, especially in the areas of initial slow crack growth, but these are less apparent in Figure 3 since lighting was adjusted to emphasize the secondary cracks (dark lines).

The results of all tests conducted in this study are summarized in Tables 1 and 2. A number of interesting observations that can be made from these data are summarized in the following paragraphs:

- (a) Quite unexpectedly, slow crack growth under constant load was found to occur about as readily in air as in saltwater, and it was apparently more extensive in air than in saltwater at high stress intensity. On the basis of macroscopic measurements of amount of slow crack growth - which are supported both by lever-arm deflection and dye marking measurements - the following comparison can be made:

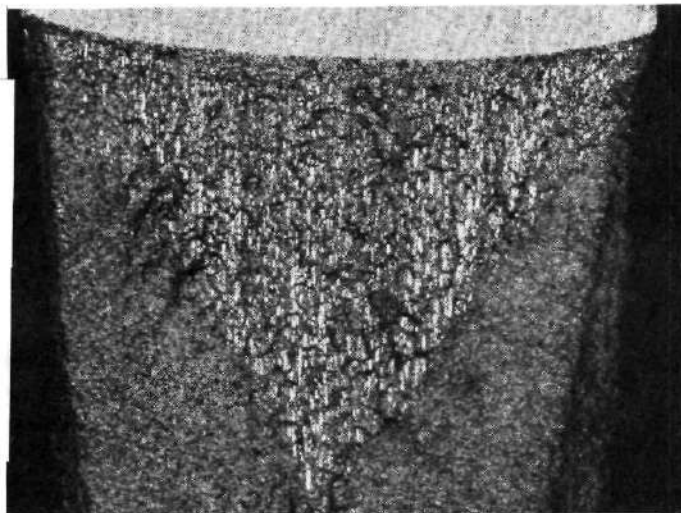
	Maximum Depth of Slow Crack Growth							
	Ti-4Al-1.5Mo-1.5V				Ti-4Al-3Mo-1V			
	Air		Saltwater		Air		Saltwater	
	Mm	In.	Mm	In.	Mm	In.	Mm	In.
72 MN/m ^{3/2} (65 ksi-in. ^{1/2})	4.7	0.185	0.3	0.012	2.5-5.3	0.1-0.208	0.6	0.025
50 MN/m ^{3/2} (45 ksi-in. ^{1/2})	0	0	0.1	0.004	0.6	0.022	0.4	0.015



13X

6F948

- a. Sample 72-2:
Loaded for 10^4 minutes
at $61 \text{ MN/m}^{3/2}$ ($55 \text{ ksi-in.}^{1/2}$) saltwater and then
rapidly loaded to failure
in air.

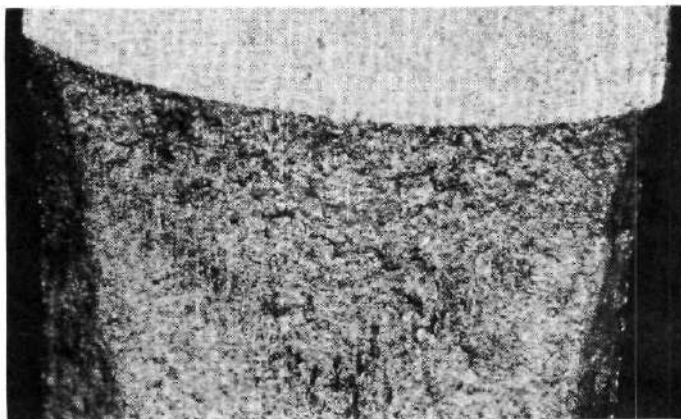


NOT REPRODUCIBLE

13X

6F949

- b. Sample 72-3:
Loaded for 10^4 minutes
at $72 \text{ MN/m}^{3/2}$ ($65 \text{ ksi-in.}^{1/2}$) in air and then
rapidly loaded to failure.



13X

6F947

- c. Sample 72-A:
Step-loaded to failure in
saltwater after prolonged
static loading at 61 to
 $78 \text{ MN/m}^{3/2}$ (55 to 70
 $\text{ksi-in.}^{1/2}$).

FIGURE 3. MACROPHOTOGRAPHS OF FRACTURE SURFACE IN
REGION OF SLOW CRACK GROWTH

TABLE 1. SUMMARY OF TESTS ON Ti-4Al-1.5Mo-0.5V ALLOY

Sample	Environment	Loading Sequence	Stress Intensity for Failure		Increase in Lever Arm Deflection, 10 ⁴ minutes	Crack Depth				
			MN/m ^{3/2}	Ksi-in. ^{1/2}		Dye Marker		Macroexamination		
						Millimeter	Inch	Millimeter	Inch	
72-F	Air	Step load to failure	92.5	83.4	--	--	--	3.2 ^(a)	0.125 ^(a)	
72-3	Air	10 ⁴ min at 72 MN/m ^{3/2} (65 ksi-in. ^{1/2}), rapid load to failure	--	--	7.0	4.6	0.18	4.7	0.185	
72-C	Air	10 ⁴ min at 50 MN/m ^{3/2} (45 ksi-in. ^{1/2}), rapid load to failure	--	--	0	0	0	0	0	
72-E	Saltwater	240 min at 50 MN/m ^{3/2} (45 ksi-in. ^{1/2}), step load to failure	98.7	89.0	--	--	--	3.6	0.142	
72-A	Saltwater	10 ⁴ min at 61 MN/m ^{3/2} (55 ksi-in. ^{1/2}), 10 ⁴ min at 67 MN/m ^{3/2} (60 ksi-in. ^{1/2}), 10 ⁴ min at 78 MN/m ^{3/2} (70 ksi-in. ^{1/2}), step load to failure	98.1	88.4	0.9 at 67 MN/m ^{3/2} (60 ksi-in. ^{1/2}) 0.8 at 78 MN/m ^{3/2} (70 ksi-in. ^{1/2})	--	--	2.9	0.115	
72-G	Saltwater	10 ⁴ min at 72 MN/m ^{3/2} (65 ksi-in. ^{1/2}), rapid load to failure in air	--	--	0.5	1.7 ^(b)	0.05 ^(b)	0.3	0.012	∞
72-2	Saltwater	10 ⁴ min at 61 MN/m ^{3/2} (55 ksi-in. ^{1/2}), rapid load to failure in air	--	--	1.7	2.5 ^(b)	0.10 ^(b)	1.5	0.058	
72-1	Saltwater	10 ⁴ min at 50 MN/m ^{3/2} (45 ksi-in. ^{1/2}), rapid load to failure in air	--	--	0.5	1.0 ^(b)	0.04 ^(b)	0.2	0.008	
72-H	Saltwater	10 ⁴ min at 50 MN/m ^{3/2} (45 ksi-in. ^{1/2}), rapid load to failure in air	--	--	0	0	0	0	0	
72-B	Saltwater	10 ⁴ min at 50 MN/m ^{3/2} (45 ksi-in. ^{1/2}), step load to failure in air	95.0	85.7	1.2	--	--	2.4 ^(a)	0.095 ^(a)	
72-D	Saltwater	10 ⁴ min at 39 MN/m ^{3/2} (35 ksi-in. ^{1/2}), step load to failure in air	97.9	88.3	0.4	--	--	1.8 ^(a)	0.070 ^(a)	
72-4	Saltwater	10 ⁴ min at 39 MN/m ^{3/2} (35 ksi-in. ^{1/2}), rapid load to failure in air	--	--	0.4	0.3	0.01	0.1	0.003	

(a) Indistinct boundary typical of step-loaded samples. Value may be in error.

(b) Some evidence of dye movement. Value may be high.

TABLE 2. SUMMARY OF TESTS ON Ti-4Al-3Mo-1V

Sample	Environment	Loading Sequence	Stress Intensity for Failure		Increase in Lever Arm Deflection, 10^4 minutes	Crack Depth			
			MN/m ^{3/2}	Ksi-in. ^{1/2}		Dye Marker		Macroexamination	
						Millimeter	Inch	Millimeter	Inch
70-D	Air	10^3 min at 72 MN/m ^{3/2} (65 ksi-in. ^{1/2}), rapid load to failure	--	--	3.1 ^(a)	2.5	0.10	2.5	0.100
70-1	Air (dried)	10^4 min at 72 MN/m ^{3/2} (65 ksi-in. ^{1/2}), rapid load to failure	--	--	7.8	5.3	0.21	5.3	0.208
70-F	Acetone	10^3 min at 72 MN/m ^{3/2} (65 ksi-in. ^{1/2}), rapid load to failure	--	--	1.8 ^(a)	1.0	0.04	1.1	0.045
70-B	Air	10^3 min at 61 MN/m ^{3/2} (55 ksi-in. ^{1/2}), 10^3 min at 67 MN/m ^{3/2} (60 ksi-in. ^{1/2}), rapid load to failure	--	--	1.2 at 67 MN/m ^{3/2} (60 ksi-in. ^{1/2}) ^(a) 0.2 at 61 MN/m ^{3/2} (55 ksi-in. ^{1/2}) ^(a)	0.8	0.03	0.4	0.015
70-3	Air (dried)	10^4 min at 50 MN/m ^{3/2} (45 ksi-in. ^{1/2}), rapid load to failure	--	--	0.3	0.5	0.02	0.6	0.022
70-A	Saltwater	10^4 min at 61 MN/m ^{3/2} (55 ksi-in. ^{1/2}), 10^4 min at 67 MN/m ^{3/2} (60 ksi-in. ^{1/2}), 10^4 min at 67 MN/m ^{3/2} (70 ksi-in. ^{1/2}), step load to failure	85.2	76.7	1.4 at 67 MN/m ^{3/2} (60 ksi-in. ^{1/2}) 2.3 at 78 MN/m ^{3/2} (70 ksi-in. ^{1/2})	--	--	3.3 ^(b)	0.130 ^(b)
70-4	Saltwater	10^3 min at 78 MN/m ^{3/2} (70 ksi-in. ^{1/2}), fractured under load	78.0 ^(c)	70.0 ^(c)	Considerable ^(c)	--	--	5.3	0.208
70-E	Saltwater	10^3 min at 72 MN/m ^{3/2} (65 ksi-in. ^{1/2}), rapid load to failure in air	--	--	0.2 ^(a)	0.5	0.02	0.6	0.025
70-C	Saltwater	10^3 min at 61 MN/m ^{3/2} (55 ksi-in. ^{1/2}), 10^3 min at 67 MN/m ^{3/2} (60 ksi-in. ^{1/2}), rapid load to failure in air	--	--	1.2 at 67 MN/m ^{3/2} (60 ksi-in. ^{1/2}) ^(a) 0.2 at 61 MN/m ^{3/2} (55 ksi-in. ^{1/2}) ^(a)	--	--	0.4	0.015
70-2	Saltwater	10^4 min at 50 MN/m ^{3/2} (45 ksi-in. ^{1/2}), rapid load to failure in air	--	--	0.5	0.3	0.01	0.4	0.015

(a) Measured after 10^3 minutes.

(b) Rather indistinct boundary between regions of slow crack growth and final fracture, which is typical of step-loaded samples. Nonsymmetrical cracking occurred and the crack was much deeper on one side of the sample.

(c) Fracture under static load at some time between 480 and 1440 minutes.

- (b) The critical stress intensity for slow crack growth in saltwater and in air was not defined by these studies. However, it is almost certainly below $50 \text{ MN/m}^{3/2}$ ($45 \text{ ksi-in.}^{1/2}$) in both alloys. Some evidence of crack growth in Ti-4Al-1.5Mo-0.5V was seen in saltwater at a stress intensity of $39 \text{ MN/m}^{3/2}$ ($35 \text{ ksi-in.}^{1/2}$). Both alloys showed crack growth in saltwater at $50 \text{ MN/m}^{3/2}$ ($45 \text{ ksi-in.}^{1/2}$) and the Ti-4Al-3Mo-1V alloy also showed crack growth in air at $50 \text{ MN/m}^{3/2}$ ($45 \text{ ksi-in.}^{1/2}$).
- (c) Slow crack growth was quite erratic. Data for four tests run on Ti-4Al-1.5Mo-0.5V at one stress-intensity level in saltwater are shown in Figure 4. Two samples showed no evidence of slow crack growth, one after 240 minutes and one after 10,000 minutes, a third sample showed crack initiation after 50 minutes and arrest after 3000 minutes, and a fourth showed initiation after 1000 minutes and arrest after 1500 minutes. Increased stress intensity appeared to increase the amount of slow crack growth although this trend is also somewhat variable, apparently another indication of the erratic nature of slow crack growth.
- (d) Failure under constant load occurred in only one sample (70-4), a Ti-4Al-3Mo-1V sample loaded at $78 \text{ MN/m}^{3/2}$ ($70 \text{ ksi-in.}^{1/2}$) in saltwater in which failure occurred at an undetermined time between 480 and 1440 minutes after loading. A small amount of external (surface) crack movement was seen in two samples loaded at high stress intensities in air (72-3 and 70-1) and undoubtedly also occurred in the sample which failed while stressed in saltwater (70-4). Macroscopic examination indicated that the external crack movement occurred by ductile rupture rather than by slow crack growth in the surface region. No facets were seen in the area immediately below the surface in the material separated during slow surface crack extension. This supports the observation that the type of stress distribution (plane stress versus plane strain) is of considerable significance in slow crack growth. Since the extent of slow crack growth increased with increased stress intensity, the absolute level of normal stress rather than the percent of plane strain loading at the crack front presumably controls the extent of slow crack growth. Crack arrest apparently results when the normal stress is reduced below some critical level by crack movement, which acts to increase the plane stress character of the crack front more rapidly than it acts to increase the stress-intensity level.
- (e) As shown by data presented in Table 3, there was no evidence of dependence of either crack initiation or crack arrest time on stress intensity.
- (f) Attempts to eliminate moisture in the air as a source of stress corrosion - by enclosing the sample in an airtight container filled with a dessicant (70-1 and 70-3) or performing the test in acetone (70-F), which is not corrosive to high-aluminum titanium-aluminum alloys - did not appear to reduce crack growth significantly.

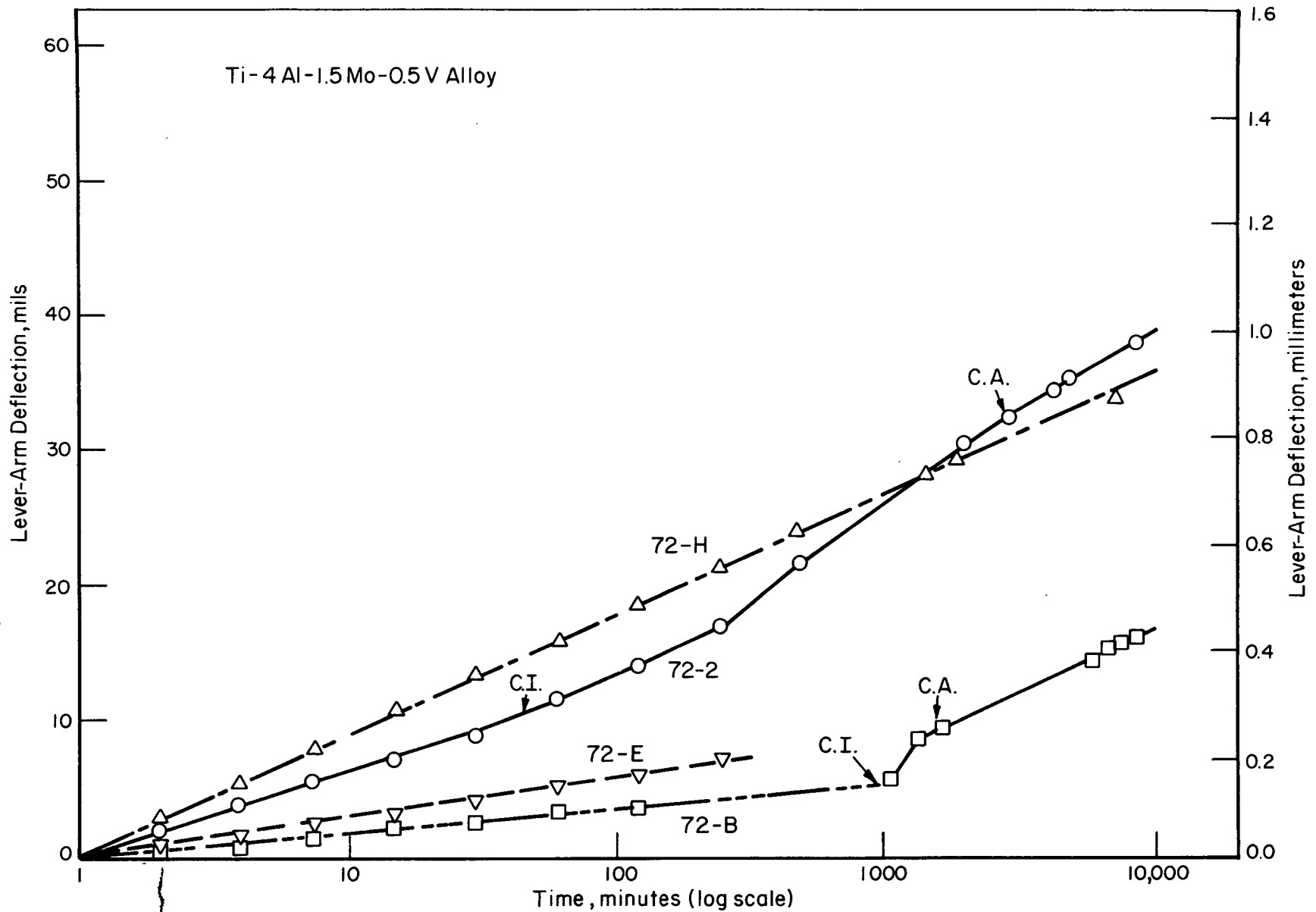


FIGURE 4. LEVER-ARM DEFLECTION OBSERVED IN FOUR PRESUMABLY IDENTICAL SAMPLES TESTED IN SALTWATER AT A STRESS INTENSITY OF $50 \text{ NM/M}^{3/2}$ ($45 \text{ KSI-IN.}^{1/2}$)

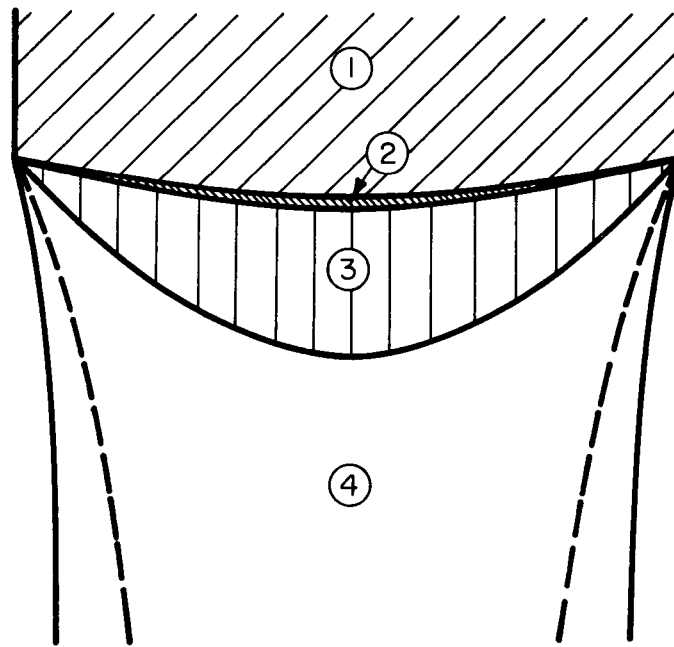
TABLE 3. CRACK-INITIATION AND CRACK-ARREST TIMES

Sample	Alloy Composition	Environment	Stress Intensity		Observed Time, minutes, for	
			MN/m ^{3/2}	Ksi-in. ^{1/2}	Crack Initiation	Crack Arrest
72-3	Ti-4Al-1.5Mo-0.5V	Air	72	65	5	200
72-C	Ditto	Air	50	45	Not observed	--
72-G	"	Saltwater	72	65	10	1,500
72-2	"	Saltwater	61	55	10	400
72-1	"	Saltwater	50	45	50	3,000
72-E	"	Saltwater	50	45	>240	--
72-H	"	Saltwater	50	45	Not observed	--
72-B	"	Saltwater	50	45	1000	1,500
72-D	"	Saltwater	39	35	300	>10,000
72-4	"	Saltwater	39	35	30	>10,000
70-D	Ti-4Al-3Mo-1V	Air	72	65	4	1,000
70-1	Ditto	Air (dried)	72	65	20	>>200
70-F	"	Acetone	72	65	3	300
70-B	"	Air	67(a)	60(a)	30	1,000
70-B	"	Air	61	55	6	500
70-3	"	Air (dried)	50	45	75	3,000
70-4	"	Saltwater	78(b)	70(b)	20	--
70-E	"	Saltwater	72	65	8	40
70-C	"	Saltwater	67(a)	60(a)	15	250
70-C	"	Saltwater	61	55	100	>1,000(?)
70-2	"	Saltwater	50	45	8	500

(a) Initially stressed for 10³ minutes at 61 MN/m^{3/2} (55 ksi-in.^{1/2}).

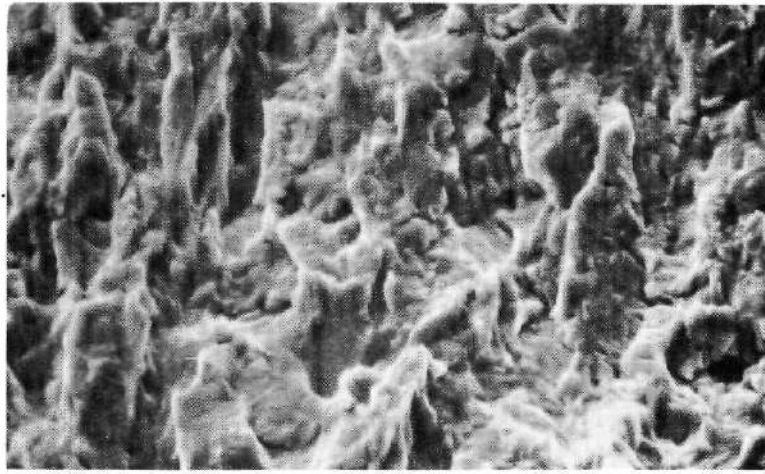
(b) Failed under constant load.

Macroexamination of the fracture surfaces showed four distinct regions to exist in these samples as illustrated schematically in Figure 5. Examination of the fracture surface of selected samples using the scanning electron microscope indicated more clearly the characteristics of these different areas. Figure 6 shows three of these regions (1, 3, and 4) in a Ti-4Al-1.5Mo-0.5V sample which was stressed in air at $72 \text{ MN/m}^{3/2}$ ($65 \text{ ksi-in.}^{1/2}$). Of particular interest is the distinctive appearance of the slow crack growth region. Stringers of cleavage fracture are seen parallel with the direction of crack movement throughout Region 3. The cleavage stringers were separated by areas of ductile fracture. Slow crack growth in this alloy apparently occurs according to the stress-corrosion crack propagation model previously proposed for high-aluminum titanium-aluminum alloys [see Figure 28, Nov. 20, 1970, Annual Summary Report on Contract NASr-100(09)]. The areas of ductile failure in Region 3 are not greatly different in appearance from the ductile failure observed in Region 4. Figure 7 shows photographs of selected regions in a sample which exhibited slow crack growth in saltwater. No obvious differences were observed in the fracture appearance in Region 3 in saltwater as compared with that in air. Either both environments introduce a similar stress-corrosion cleavage failure mode, or cleavage failure is not a result of stress corrosion. Figure 7 includes two photographs of an area at the boundary between Regions 2 and 3. The distinguishing features of Region 2 are extreme roughness and an absence of cleavage fracture patches.



- (1) Fatigue-crack.
- (2) Region of fast crack growth on load application.
- (3) Region of slow crack growth under constant or slowly rising load.
- (4) Region of final rapid fracture.

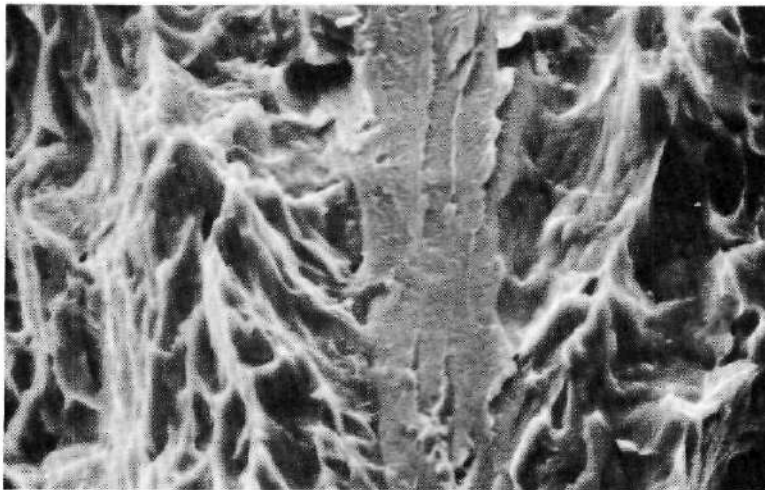
FIGURE 5. SCHEMATIC REPRESENTATION OF FRACTURE SURFACE
Compare with Figure 3a.



1000X

S-5862

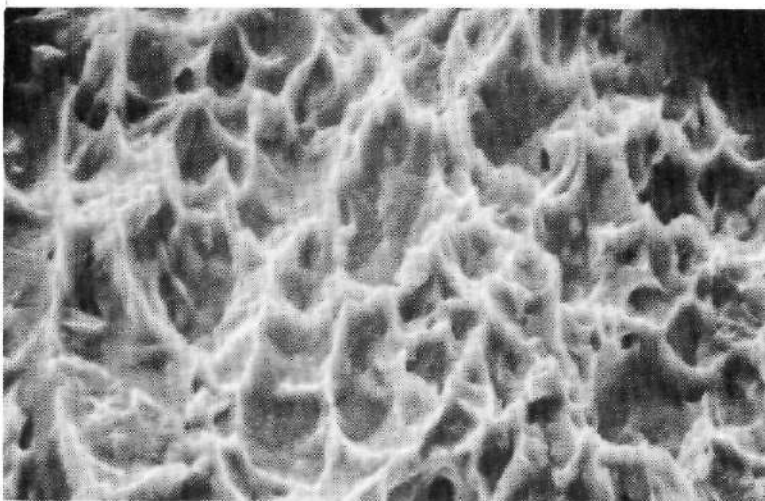
a. Fatigue Crack, Region 1



1000X

S-5863

b. Slow Crack Growth, Region 3



1000X

S-5866

c. Fast Fracture, Region 4

FIGURE 6. FRACTURE SURFACE OF Ti-4Al-1.5Mo-0.5V LOADED AT $72 \text{ MN/m}^{3/2}$ ($65 \text{ KSI-IN.}^{1/2}$) IN AIR (72-3)
 Direction of crack movement is vertical.

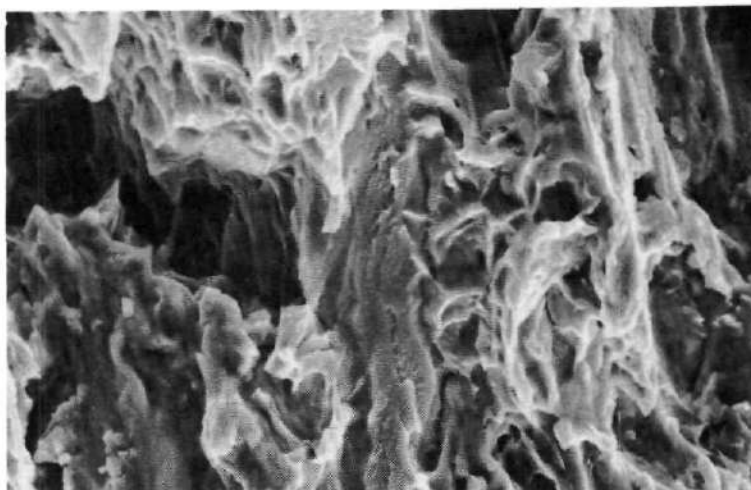
BATTELLE - COLUMBUS



200X

S-5874

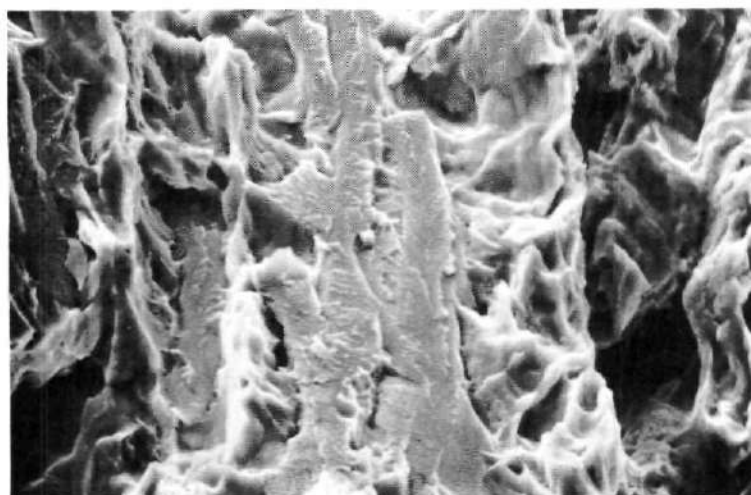
a. Boundary Between Regions 2 and 3



1000X

S-5873

b. Boundary Between Regions 2 and 3



1000X

S-5867

c. Slow Crack Growth, Region 3

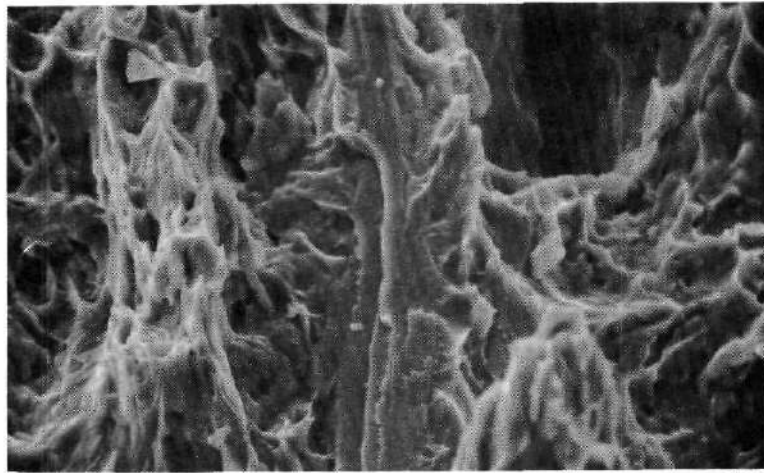
FIGURE 7. FRACTURE SURFACE OF Ti-4Al-1.5Mo-0.5V STRESSED AT $61 \text{ MN/m}^{3/2}$ ($55 \text{ KSI-IN.}^{1/2}$) IN SALTWATER (72-2)
 Direction of crack movement is vertical.

Figure 8 shows the transition in structure in the slow crack growth region of a sample which was stressed in saltwater for periods of 10^4 minutes at 61, 67, and 78 $\text{MN}/\text{m}^{3/2}$ (55, 60, and 70 $\text{ksi-in.}^{1/2}$) and was then step loaded over approximately a 5-hour period to failure at 98.1 $\text{MN}/\text{m}^{3/2}$ (88.4 $\text{ksi-in.}^{1/2}$). The initial portion of Region 3 was typical of the slow crack structure already described and probably represents crack movement under constant load at stress intensities between 61 and 78 $\text{MN}/\text{m}^{3/2}$ (55 and 70 $\text{ksi-in.}^{1/2}$). Deeper in the slow crack regions the amount of cleavage fracture decreases. This probably represents failure occurring during step loading in which, because of the higher stress intensity, less cleavage fracture is necessary before ductile overload failure will occur between the cleavage stringers. The third photograph shows an area near the end of Region 3 which contained secondary cracks, one of which is seen in this photograph running approximately vertically. Secondary cracking of this type is common in high-aluminum titanium-aluminum alloys which have failed under constant load in saltwater.

The microstructure of Ti-4Al-1.5Mo-0.5V as observed by optical microscopy in a plane parallel with the fracture surface is shown in Figure 9. Comparison with the fracture surfaces shown by scanning electron microscopy suggests the possibility that the regions of cleavage separation may correlate with regions of apparently similarly oriented stringered alpha grains, as indicated in Figure 5 by regions showing continuous beta grain boundary material and an absence of well developed alpha grain boundaries.

Several interesting conclusions can be based upon the results of this investigation:

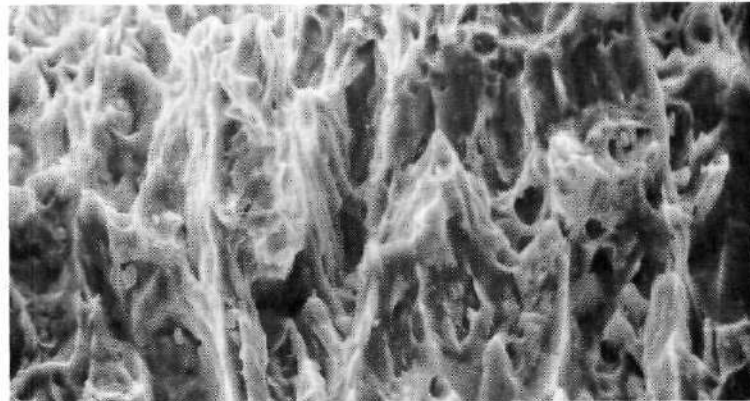
- (a) Low-aluminum titanium-aluminum alloys are susceptible to slow crack growth under sustained loading in the presence of a sharp notch. The structural features of the slow crack-growth region are similar to those observed in high-aluminum alloys exposed to saltwater stress corrosion. Slow crack growth occurs at quite low stress intensities, at least as low as 50 $\text{MN}/\text{m}^{3/2}$ (45 $\text{ksi-in.}^{1/2}$), in both Ti-4Al-1.5Mo-0.5V and Ti-4Al-3Mo-1V alloys.
- (b) Slow crack growth in these alloys occurs in both saltwater and air. The structural features of the slow crack region induced in either environment appear identical. If slow crack growth is attributed to stress corrosion, air is as aggressive an environment as saltwater in the case of these alloys. Attempts to exclude moisture as a factor in air tests did not affect slow crack growth behavior, but it is possible that the experimental procedures were inadequate.
- (c) Crack arrest occurs in 6.34 mm- (0.25-inch) thick samples under sustained loading at an initial stress intensity of 72 $\text{MN}/\text{m}^{3/2}$ (65 $\text{ksi-in.}^{1/2}$) or less. Arrest occurred both in air and in saltwater. Crack arrest is apparently related to the reduction in normal stress developed at the crack front accompanying the transition from a plane strain to a plane stress distribution as slow crack growth occurs.
- (d) The initiation of crack growth is quite erratic. Although growth usually started within 10 minutes of load application, delay periods of as long as 1000 minutes were noted. Crack growth rates and depths at the point of arrest were also highly variable and did not correlate well with initial stress intensity.



1000X

S-5889

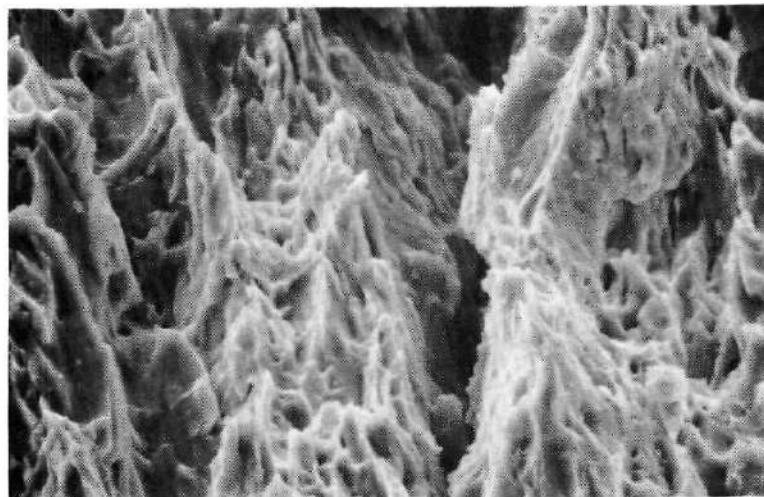
a. Initial Portion of Region 3



1000X

S-5887

b. Intermediate Portion of Region 3



1000X

S-5883

c. Final Portion of Region 3

FIGURE 8. FRACTURE SURFACE OF Ti-4Al-1.5Mo-0.5V SAMPLE STRESSED AT 61 TO 78 MN/m^{3/2} (55 TO 70 KSI-IN.^{1/2}) FOR 3 x 10⁴ MINUTES AND THEN STEP LOADED TO FAILURE IN SALTWATER (72-A)

Direction of crack movement is vertical.

BATTELLE - COLUMBUS

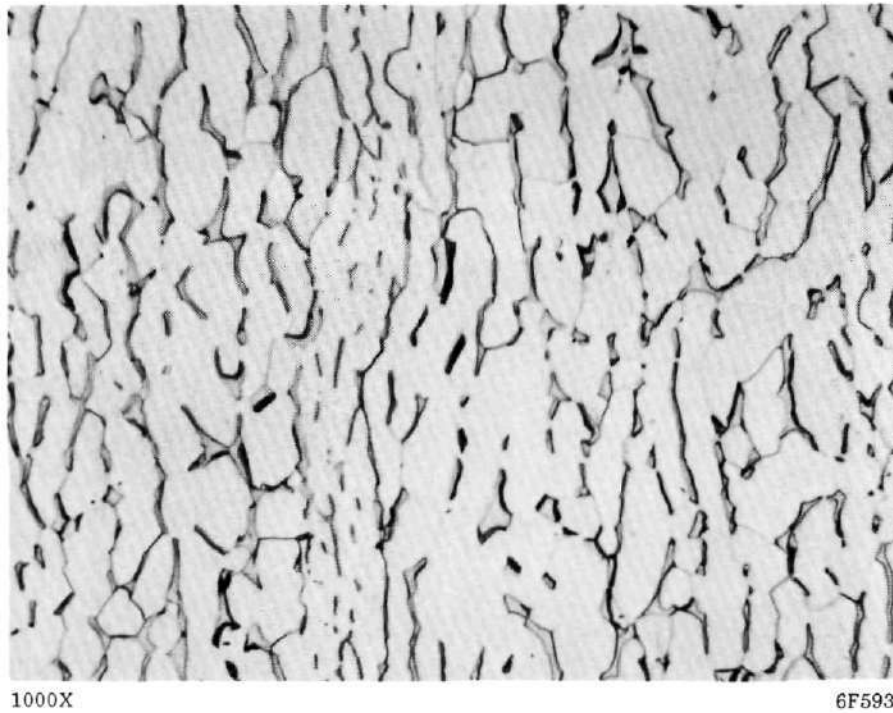
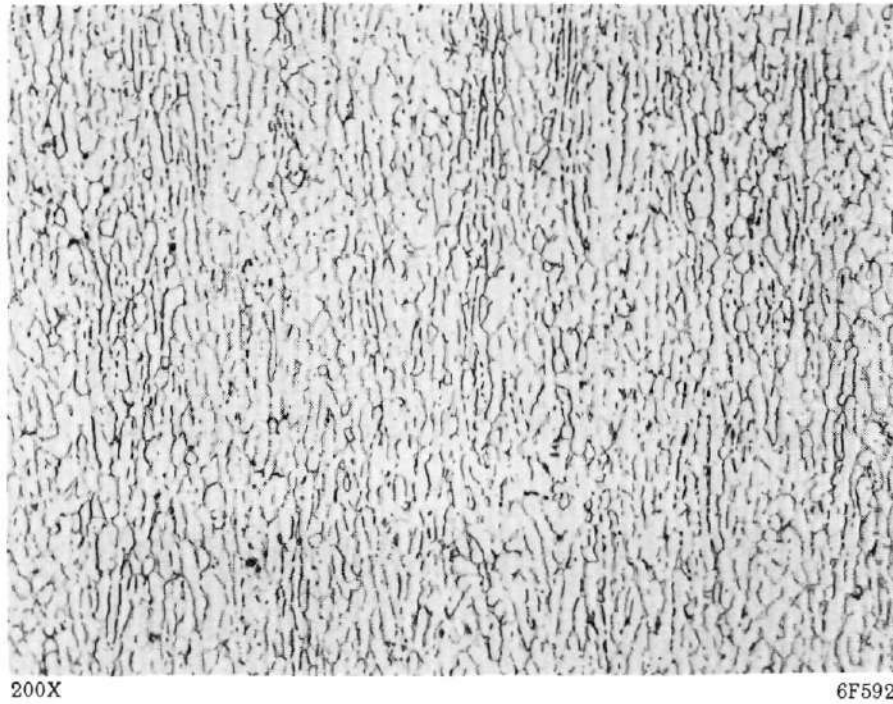


FIGURE 9. MICROSTRUCTURE OF Ti-4Al-1.5Mo-0.5V (72-2) IN A PLANE PARALLEL WITH THE FRACTURE SURFACE SHOWN IN FIGURES 6 THROUGH 8

Direction of crack propagation is vertical.

- (e) Appreciable slow crack growth can occur internally with no visible evidence of crack propagation on the surface. Surface propagation of cracks in these alloys results from ductile failure of the surface region after extensive unseen internal slow crack growth. In 6.34 mm- (0.25-inch) thick samples of the two moderate-strength alloys examined in this study, internal cracking proceeded to a depth of over 2.5 mm (0.1 inch) before any evidence of surface crack extension was seen.

METALLURGICAL MECHANISMS OF STRESS-CORROSION CRACKING

It is well established that the susceptibility of titanium-aluminum-base alloys to aqueous stress-corrosion cracking increases with an increasing volume fraction of Ti_3Al . In certain cases, the precipitation of Ti_3Al can render an otherwise immune alloy susceptible to crack initiation and growth in saltwater. (1) It is also well known that Ti_3Al reduces the fracture toughness of titanium-aluminum-base alloys, and there is some evidence that the size distribution of the Ti_3Al particles has a significant effect on the degree of embrittlement in air (2) and in saltwater (3). Accordingly, in the present research program the relation between the size distribution of Ti_3Al precipitates and slip character, fracture toughness, and susceptibility to aqueous stress-corrosion cracking is being studied in Ti-8Al.

To date, only those heat treatments which produce very small Ti_3Al particles (mean diameter = 25-50 Å) have been investigated. Such heat treatments do not have a significant effect on yield stress or tensile ductility but do render an alloy susceptible to aqueous stress-corrosion cracking. There is evidence that during plastic deformation the long-range-ordered structure of the Ti_3Al particles is completely destroyed in the vicinity of slip bands. Furthermore, narrow depressions or "trenches" are often observed where slip bands intersect the surface of a specimen. It is thought that the enhanced chemical potential of the slip bands leads to localized anodic dissolution of the slip steps, which ultimately results in a macroscopic stress-corrosion crack. During the next research period, specimens of Ti-8Al containing much larger Ti_3Al particles will be investigated. Specimens have been aged at 600 and 650 C to produce the appropriate size distributions of Ti_3Al particles. These specimens will be deformed in air and saltwater, and the slip character will be studied by replica and transmission electron microscopy as before.

REFERENCES

- (1) J. D. Boyd and R. G. Hoagland, "The Relation Between Surface Slip Topography and Stress-Corrosion Cracking in Ti-8 wt. % Al", presented at the International Symposium on Stress Corrosion Mechanisms in Ti Alloys, Atlanta, Georgia, 1971, to be published by NACE.

- (2) G. Lütjering and S. Weissmann, "Mechanical Properties of Age-Hardened Titanium-Aluminum Alloys", *Acta Met.*, 18, 785 (1970).
- (3) J. L. Cavallaro and R. C. Wilcox, "Embrittlement of Ti-7Al Binary Alloy in Sea Water", *Corrosion*, 27, 157 (1971).

DNW:RAW:JDB:RIJ/jbs